# Clusters of Group II−VI Materials: $Cd_iO_i$ ($i \leq 15$)

## Jon M. Matxain,* Jose M. Mercero, Joseph E. Fowler, and Jesus M. Ugalde

*Kimika Fakultatea, Euskal Herriko Unibertsitatea, P.K. 1072, 20018 Donostia, Euskadi (Spain)*

*Received: May 6, 2003; In Final Form: September 5, 2003*

In this work, the ground states of $Cd_iO_i$ clusters ($i = 1-9, 12, 15$) are studied. Ringlike structures have been found to be the global minima for clusters as large as $i = 7$, and three-dimensional structures (clustertubes and spheroids) are observed to be the global minima for larger ones ($i = 8, 9, 12, 15$). This trend has been ascribed to the stability of obtuse O−Cd−O angles in the first case, and to the stability gained from higher coordination in the second case. The three-dimensional structures may be envisioned as being built from $Cd_2O_2$ and $Cd_3O_3$ rings, as it is the case for $Zn_iX_i$ (where X = O, S, Se, Te) three-dimensional structures. Calculated cohesive energies increase as the cluster size increases, which gives support to the idea that the predicted global minima are the correct ones.

## 1. Introduction

Semiconductors are materials of great importance in the development of technology. The computer revolution and other technological devices have been (and are) in rapid development, basically because of improved semiconductor materials. Some of these materials are the group II−VI compounds, whose interest has increased notably, because of their paramount technological potential. Applications such as photovoltaic solar cells,[1−10] optical sensitizers,[11] photocatalysts,[12,13] or quantum devices[14] have led to extensive investigation. To understand these phenomena, it is essential to study the structure and electronic properties of these compounds, thereby providing more information about the optimization of these materials to enhance their applicability. Many theoretical studies have been reported concerning the electronic structure of these semiconductor compounds.[15−22]

Nevertheless, there are some properties related to these compounds that have been observed to be local phenomena. That is, when they happen, they happen in a certain well-defined domain. Thus, it is important to study small clusters of these compounds, whose electronic and structural properties could give insight into understanding these local properties, including their catalytic behavior.[23] Also, the fact that cluster and nanoparticle characterization is becoming technologically feasible is remarkable. This makes cluster science more interesting, because, in addition to its capability in helping to rationalize some of their surface-related properties, studies of clusters of increasingly larger size can eventually fill the gap with the nanosized-materials domain in a comprehensible manner. As a matter of fact, experimental studies on nanoparticles 2−3 nm in diameter are becoming routine.[24,25] Concomitantly, it is worth noting that the diameter of $Cd_{15}O_{15}$ is 0.85 nm. Thus, several experimental[26−33] and theoretical[34−38] studies have been reported concerning clusters of various compositions, which have important and interesting applications.

Therefore, the study of small group II−VI clusters seems to be promising. Experimentally, nanoparticles of a variety of compounds have been recently grown, including CdS,[39]

* Author to whom correspondence should be addressed. E-mail: pobmabej@sq.ehu.es.

CdSe,[40−43] and ZnO.[44] The diameter of the smallest observed particles lie between 0.9 and 3 nm for CdSe, while the smallest ZnO particles are 3 nm in diameter. Theoretical calculations performed previously in our group for $Zn_iS_i$ ($i = 1-9$),[45] $Zn_iO_i$ ($i = 1-9$),[46] and $Zn_iSe_i$ and $Zn_iTe_i$ ($i = 1-9$)[47] clusters show structures similar to these sizes, which means that the available theoretical and experimental data almost match. Indeed, we have been able to characterize spheroid structures with a diameter of 0.85 nm, which is similar to the experimentaly smallest detected group II−VI nanoparticle.[40] Spheroid fullerene-type structures were the global minima for $i \geq 6$ for $Zn_iS_i$, $Zn_iSe_i$, and $Zn_iTe_i$, and $i \geq 8$ for $Zn_iO_i$, which is in accordance with previous molecular dynamics calculations.[48]

The study of the structures and properties of these $Cd_iO_i$ clusters may open a new window in the applications of these materials, because the cluster properties will differ significantly from the bulk ones. New materials could be developed in this way.

## 2. Method

All geometries were fully optimized using the hybrid[49] Becke 3 Lee−Yang−Perdew (B3LYP) gradient-corrected approximate density functional procedure.[50−52] Harmonic vibrational frequencies were determined by analytical differentiation of the gradients.

The relativistic compact effective core potentials and shared-exponent basis set[53] of Stevens, Krauss, Basch, and Jasien (SKBJ), including the 4d electrons of Cd in the valence, were used as the basic basis set in this study. For the geometry optimizations and harmonic frequency calculations, an extra d function was added on Cd ($\alpha = 0.23$) and O ($\alpha = 0.85$), because of their importance for the proper description of the high coordination of the atoms in the three-dimensional cluster structures. We denote this basis set as SKBJ(d). To obtain accurate relative energies, single-point calculations were performed using an expanded SKBJ(d) basis set, denoted as SKBJ-(expan). The exponents may be seen in Table 1. This basis set was too large to use to perform the geometry optimizations.

The exponents of all these added functions were energy optimized, using the GAMESS package.[54] Note that pure angular
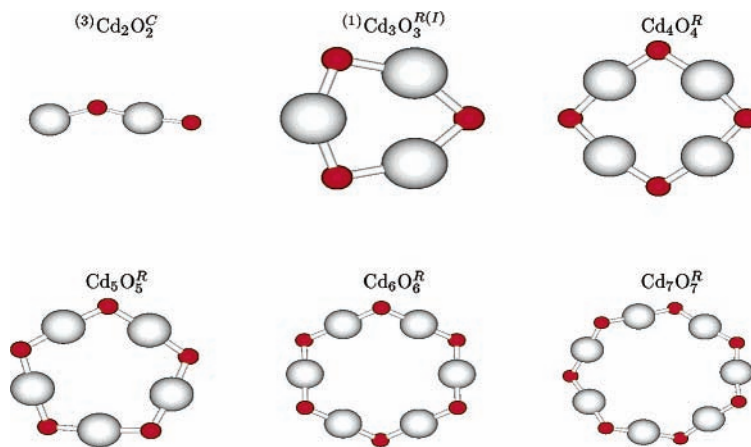
**Figure 1.** Calculated global minima of Cd$_i$O$_i$, $i = 2$−7. The dark smaller atoms represent oxygen.

**TABLE 1: SKBJ(expan) Basis Set for Cd and O Atoms**

| | Cd | | | O | | |
|---|---|---|---|---|---|---|
| | a | d | d | a | d | d |
| sp | 0.261148 | 1.0 | 1.0 | 1.206642 | 1.0 | 1.0 |
| sp | 0.18201 | 1.0 | 1.0 | 0.561051 | 1.0 | 1.0 |
| d | 1.350188 | 1.0 | | 2.179302 | 1.0 | |
| d | 0.23 | 1.0 | | 0.628849 | 1.0 | |
| d | 0.097397 | | | | | |
| f | 1.451 | 1.0 | | 1.666029 | 1.0 | |
| f | 0.326695 | 1.0 | | | | |

momentum functions were used throughout this study. We denote the final basis set used as SKBJ(d).

Because there are so many possible structures for these clusters, several starting points for these complete B3LYP/ SKBJ(d) optimizations were generated, using a simulated annealing approach at the PM3[55] level of theory. Of course, additional starting points were derived from simple chemical intuition. We must mention that the large amount of structures that appear as the cluster size increases makes the study of all of them impossible. In this study, only some structures of each size have been considered.

All the geometry optimizations and frequency calculations were performed with the GAUSSIAN 98[56] package. For the PM3 simulated annealing technique, the HYPERCHEM[57] program was used.

## 3. Results

**3.1. Structures of Characterized Minima of Cd$_i$O$_i$ ($i =$ 1−9, 12, 15).** In this section, the predicted minima are described. Although our interest focuses on the global minima, structures and properties of higher-lying local minima are also presented.

We have divided these clusters in two groups, according to the geometrical shape of the global minimum. In Group 1, Cd$_i$O$_i$ ($i = 1$−7) clusters are included, the global minima of which are planar or near-planar ringlike structures. The remaining Cd$_i$O$_i$ clusters, for which the global minima are three-dimensional structures, are categorized in the second group, Group 2. The characterized structures belong to different families, namely rings (R), chains (C), three rings (3R), spheroids (S), distorted spheroids (D), and clustertubes (CT). The difference between spheroids and distorted spheroids will be clear later in the paper.

The presented structures are labeled according to the following scheme: $^{(s)}$Cd$_i$O$_i^a$, where ($s$) denotes the multiplicity, $i$ denotes the number of CdO units, and the superscript $a$ represents the structure family. Note that only triplet states have

been considered for small clusters, and only singlets have been considered for larger clusters. Hence, for the latter clusters, spin multiplicity will not be shown.

*3.1.1. Group 1.* In this section, the calculated structures of Cd$_i$O$_i$ ($i = 1$−7) are described. Figure 1 shows the predicted global minima of Cd$_i$O$_i$, and Figure 2 shows their corresponding local minima. Table 2 lists properties of the studied structures, such as molecular geometrical parameters, energies, and symmetry.

Triplet chain structures have been observed to be the global minima for small clusters ($i = 1, 2$), whereas ringlike triplet and singlet structures have higher energies. As the cluster size increases, the triplet states have higher energies, as can be seen for $i = 3$, where the triplet chain structure lies 30.56 kJ/mol above the singlet ring structure, per CdO unit. Thus, only singlet structures have been characterized for larger clusters. For $i \geq$ 3, the global minima structures have been observed to be planar rings ($i = 3$−4) or near-planar rings ($i = 5$−7). The main reason to break the planarity in these ring structures is the observed strong tendency to form linear O−Cd−O angles. Thus, optimized bond angles are $\alpha = 170°$−$180°$ for Cd$_i$O$_i^R$ ($i = 5$−7); concomitantly, the bond lengths decrease from $R = 2.06$ Å to $R = 1.99$ Å as the size of the ring increases. Local minima have been observed to be planar for $i = 2$−3, and three-dimensional local minima were only observed for $i = 4$−7. These three-dimensional structures can be pictured as being built from $^{(1)}$Cd$_2$O$_2^{R(I)}$ (square) and Cd$_3$O$_3^{R(I)}$ (hexagon)-like structures. Cd$_4$O$_4^S$ consists of six squares, which share atoms with each other, forming a type of deformed cube. Cd$_5$O$_5^D$ is built from four squares and two hexagons. Cd$_6$O$_6^S$ is built from two "parallel" hexagons joined together by six squares. The same building blocks are found in Cd$_6$O$_6^{3R}$, which is built from two hexagons linked by a square. Cd$_7$O$_7^{D(I)}$ can be seen as a structure of two joined Cd$_3$O$_3$ rings and one bent Cd$_4$O$_4$ ring. Half of the Cd$_4$O$_4$ ring is linked to the Cd$_3$O$_3$ ring, forming, in this way, new squares (as in Cd$_6$O$_6^S$) and a second bent Cd$_4$O$_4$ ring. Cd$_7$O$_7^{D(II)}$ is built from four squares and four hexagons. In these three-dimensional structures, the bond lengths are larger than those the rings, and angles are far from linearity, because of geometrical constraints.

Examination of the relative energies given in Table 2 shows that (i) the largest relative energy per CdO unit occurs in Cd$_4$O$_4$, and (ii) when the size increases, the energy difference between the ring structure and the spheroid structure decreases. In comparison to Zn$_i$O$_i$ clusters, where the same trend is observed, we can see that the relative energies are generally larger.
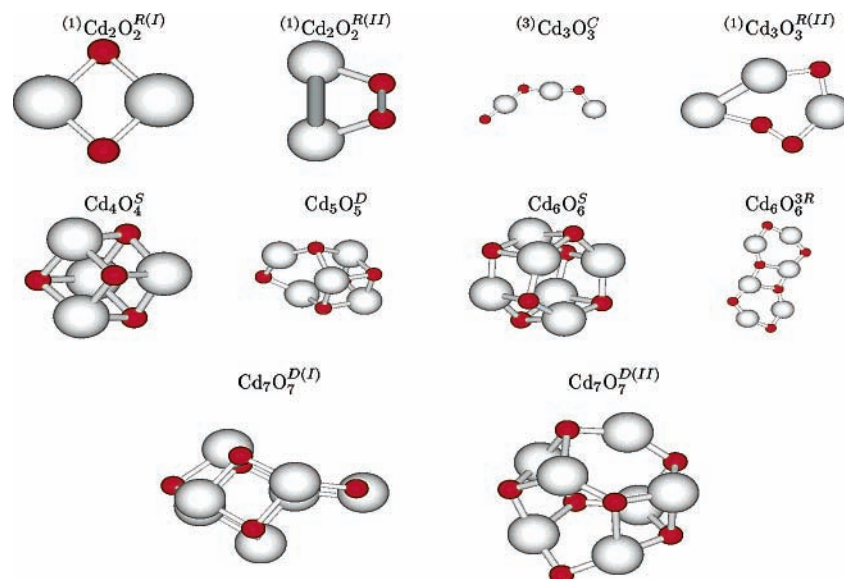
**Figure 2.** Calculated local minima of $Cd_iO_i$, $i = 2-7$.

**TABLE 2: Cd–O Bond Lengths ($R$), O–Cd–O Angles ($\alpha$), and Symmetry Groups of the Structures of Figures 1 and 2**

|  | $R$ (Cd–O) | $\alpha$ (O–Cd–O) | symmetry | $(\Delta E)/i$ (kJ/mol)[a] |
|---|---|---|---|---|
| $^{(3)}Cd_1O_1^C$ | 2.15 |  | $C_{\infty v}$ |  |
| $^{(1)}Cd_1O_1^C$ | 1.93 |  | $C_{\infty v}$ | +40.63 |
| $^{(3)}Cd_2O_2^C$ | 1.97–2.06 | 170.0 | $C_1$ |  |
| $^{(1)}Cd_2O_2^{R(I)}$ | 2.13 | 99.8 | $D_{2h}$ | +26.28 |
| $^{(1)}Cd_2O_2^{R(II)}$ | 2.31 |  | $C_{2v}$ | +29.90 |
| $^{(3)}Cd_2O_2^{R(III)}$ | 2.14 | 85.2 | $D_{2h}$ | +30.64 |
| $^{(1)}Cd_2O_2^{R(IV)}$ | 1.93–2.04 | 172.4 | $C_1$ | +62.65 |
| $^{(1)}Cd_3O_3^{R(I)}$ | 2.05 | 145.3 | $C_{2v}$ |  |
| $^{(3)}Cd_3O_3^C$ | 2.03–2.20 | 116.5–158.9 | $C_{2v}$ | +30.56 |
| $^{(1)}Cd_3O_3^{R(II)}$ | 2.05–2.57 | 131.1 | $C_s$ | +68.26 |
| $Cd_4O_4^R$ | 2.02 | 167.3 | $D_{2h}$ |  |
| $Cd_4O_4^S$ | 2.23 | 94.3–94.4 | $C_{2v}$ | +50.72 |
| $Cd_5O_5^R$ | 2.00–2.01 | 175.4–176.1 | $C_1$ |  |
| $Cd_5O_5^D$ | 2.06–2.26 | 88.3–141.3 | $C_1$ | +42.21 |
| $Cd_6O_6^R$ | 1.99–2.00 | 178.6–179.3 | $C_{2h}$ |  |
| $Cd_6O_6^S$ | 2.13–2.34 | 91.7–133.7 | $C_{2h}$ | +14.19 |
| $Cd_6O_6^{3R}$ | 2.02–2.40 | 80.8–152.5 | $C_i$ | +15.43 |
| $Cd_7O_7^R$ | 1.99 | 174.3–176.6 | $C_1$ |  |
| $Cd_7O_7^{D(I)}$ | 2.04–2.41 | 86.8–166.9 | $C_1$ | +9.42 |
| $Cd_7O_7^{D(II)}$ | 2.03–2.38 | 86.6–149.5 | $C_2$ | +16.18 |

[a] For the local minima, energies relative to the corresponding minimum are given in kJ/mol, per CdO unit.

*3.1.2. Group 2.* This group contains the clusters whose global minima are three-dimensional structures, i.e., $Cd_iO_i$ ($i = 8, 9, 12, 15$). The global minima of $Cd_iO_i$ are shown in Figure 3, and the local minima are shown in Figure 4. In Table 3, the Cd–O bond lengths ($R$), O–Cd–O angles ($\alpha$), electronic energies, and point-group symmetries of the calculated structures are given.

Three structures have been characterized for $Cd_8O_8$. $Cd_8O_8^{CT}$ may be viewed as being built from two "parallel" $Cd_4O_4$ rings linked together by $Cd_2O_2$ rings. $Cd_8O_8^S$ is a three-dimensional structure built from squares and hexagons. It may be viewed as a four-faced polyhedron where each face is built from a $Cd_2O_2$ ring and a $Cd_3O_3$ ring, which are rotated to build the next face. This structure has $Cd_2O_2$ rings at the top and bottom. Altogether,
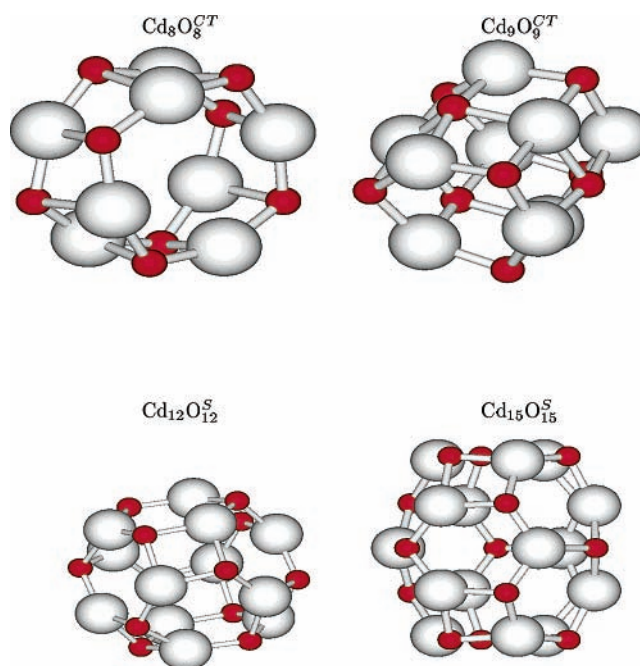


**Figure 3.** Calculated global minima of $Cd_iO_i$, $i = 8, 9, 12, 15$.

six squares and four hexagons are found in this structure. $Cd_8O_8^R$ has all the Cd atoms on the same plane, but the O atoms alternate up and down with respect to the ring's plane. Linear O–Cd–O angles are achieved in this way.

Three structures have been characterized for $Cd_9O_9$. $Cd_9O_9^{CT}$ is formed by three stacked $Cd_3O_3$ rings, linked together by $Cd_2O_2$ units. It may be constructed by adding an extra $Cd_3O_3$ ring to $Cd_6O_6^S$. $Cd_9O_9^S$ is a three-dimensional spheroid composed by squares and hexagons, as in smaller clusters. In total, there are six squares and five hexagons in this structure. Finally, $Cd_9O_9^R$ is a ring structure similar to $Cd_8O_8^R$.

Three structures have been characterized for $Cd_{12}O_{12}$. $Cd_{12}O_{12}^S$ is a three-dimensional structure built from six squares and eight hexagons. The six squares are located parallel to the $xy$, $yz$, and $xz$ planes: one in the front, one in the back, one at the left, the other at the right, one at the top, and the other at the bottom. The squares are linked by the hexagons. The $Cd_{12}O_{12}^{CT}$ may be viewed as being built by four "parallel"

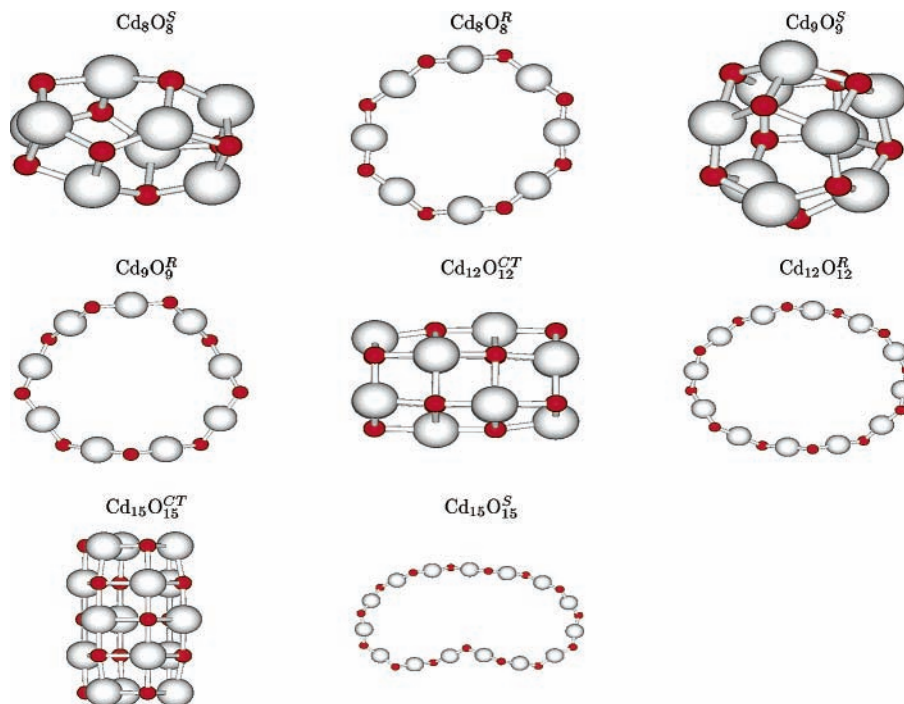**Figure 4.** Calculated local minima of $Cd_iO_i$, $i = 8, 9, 12, 15$.

**TABLE 3: Cd−O Bond Lengths ($R$), O−Cd−O Angles ($\alpha$), and Symmetry Groups of the Structures of Figures 3 and 4**

| | $R$ (Cd−O) | $\alpha$ (O−Cd−O) | symmetry | $(\Delta E)/i$ (kJ/mol)[a] |
|---|---|---|---|---|
| $Cd_8O_8^{CT}$ | 2.09−2.43 | 90.0−153.4 | $C_{4v}$ | |
| $Cd_8O_8^{S}$ | 2.10−2.29 | 89.7−134.3 | $C_2$ | +5.35 |
| $Cd_8O_8^{R}$ | 1.99 | 173.3−178.0 | $C_2$ | +6.27 |
| $Cd_9O_9^{CT}$ | 2.15−2.25 | 89.1−137.6 | $C_s$ | |
| $Cd_9O_9^{S}$ | 2.11−2.25 | 90.3−130.4 | $C_s$ | +1.68 |
| $Cd_9O_9^{R}$ | 1.99 | 178.8−179.7 | $C_1$ | +10.41 |
| $Cd_{12}O_{12}^{S}$ | 2.10−2.20 | 87.9−129.2 | $C_s$ | |
| $Cd_{12}O_{12}^{CT}$ | 2.14−2.35 | 88.5−178.1 | $C_1$ | +1.76 |
| $Cd_{12}O_{12}^{R}$ | 1.99 | 176.5−178.0 | $C_1$ | +25.16 |
| $Cd_{15}O_{15}^{S}$ | 2.15−2.25 | 88.8−136.5 | $C_s$ | |
| $Cd_{15}O_{15}^{CT}$ | 2.09−2.20 | 87.5−136.9 | $C_{3h}$ | +3.32 |
| $Cd_{15}O_{15}^{R}$ | 1.99 | 176.4−179.1 | $C_1$ | +41.10 |

[a] For the local minima, energies relative to the corresponding minimum are given in kJ/mol, per CdO unit.

**TABLE 4: Structural Trends in BN Spheroids and Fullerenes**

| | $Cd_4O_4^{S}$ | $Cd_6O_6^{S}$ | $Cd_8O_8^{S}$ | $Cd_9O_9^{S}$ | $Cd_{12}O_{12}^{S}$ | $Cd_{15}O_{15}^{S}$ |
|---|---|---|---|---|---|---|
| squares | 6 | 6 | 6 | 6 | 6 | 6 |
| hexagons | 0 | 2 | 4 | 5 | 8 | 11 |

| | $C_{20}$ | $C_{34}$ | $C_{48}$ | $C_{60}$ | $C_{72}$ | $C_{94}$ |
|---|---|---|---|---|---|---|
| pentagons | 12 | 12 | 12 | 12 | 12 | 12 |
| hexagons | 0 | 7 | 14 | 20 | 26 | 37 |

$Cd_3O_3$ rings linked together by $Cd_2O_2$ rings. This structure is similar to $Cd_9O_9^{CT}$; however, a fourth $Cd_3O_3$ ring has been added. Finally, $Cd_{12}O_{12}^{R}$ is a ring with the O atoms alternating up and down, with respect to the ring's plane.

Three structures have been characterized for $Cd_{15}O_{15}$. The global minimum is a three-dimensional structure built from 6 squares and 11 hexagons. The final result is an elongated spheroid, similar to a rugby ball. $Cd_{15}O_{15}^{CT}$ is built from five "parallel" $Cd_3O_3$ rings linked together by $Cd_2O_2$ rings, similar to $Cd_{12}O_{12}^{CT}$ with an extra $Cd_3O_3$. Finally, $Cd_{15}O_{15}^{R}$ is a disturbed ring with the O atoms placed so that the O−Cd−O angles are approximate to linearity.

In all these complexes, spheroid structures are built from squares and hexagons, with the number of squares being constant (six), whereas the number of hexagons increases as the cluster size increases. This is the so-called square−hexagon route for binary compounds and has been observed for other group II−VI and group III−V compounds. This square−

hexagon route is similar to the pentagon−hexagon route found in carbon fullerenes, as can be observed in Table 4. Distorted spheroids are spheroids that do not follow this trend.

In summary, geometrical parameters follow the trend of clusters of Group 1. Three-dimensional structures have larger bond lengths than the ring structures, whose bond lengths are similar to the rings of Group 1. In addition, linear O−Cd−O angles are found in these rings, as were found in smaller cases. For clusters of Group 1, rings have been observed to be the global minima and three-dimensional structures are the local minima. However, recall that the relative energies between these rings and three-dimensional local minima decrease as the cluster size increases. Thus, for $i = 6$, the relative energy per CdO unit was 14.19 kJ/mol, and, for $i = 7$, the relative energy decreased to 9.42 kJ/mol. Finally, for $i = 8$, the three-dimensional structure became the global minimum, having a relative energy of 6.27 kJ/mol.

The newly described three-dimensional structures are basically of two types: spheroids and clustertubes. Most of them are built from squares and hexagon building blocks, as were the three-dimensional local minima in Group 1, but the type of structures formed are different. Spheroids are structures in which the number of squares remain constant (six), whereas the number of hexagons increases as the cluster size increases. Clustertubes may be viewed as short tubes where hexagons are linked together, forming a chain of hexagons. In some cases, the tubes are observed to be the global minima ($i = 8, 9$); in other cases, the spheroids are the global minima ($i = 12, 15$). However, the

relative energies are quite small, and more-sophisticated methods (such as quantum Monte Carlo methods) could be used to confirm the obtained results.

**3.2. Comparison with Other Group II−VI Clusters.** $Zn_iX_i$ clusters have previously been studied in our group.[45−47] Related structures were found for these other clusters, but with significant differences in the global minima structures. Ring structures, where linear X−Zn−X and O−Cd−O angles are favored, are observed to be the global minima for $Zn_iO_i$ and $Cd_iO_i$ ($i \leq 7$ clusters). However, for the remaining combinations, $Zn_iX_i$ (X = S, Se, Te) rings are the global minima for $i \leq 5$ clusters. This may be explained by the greater ability of S, Se, and Te atoms to achieve high coordination, because of the d orbitals, which, however, are very high in energy for O atoms. The planarity of these rings is broken, to achieve the linearity of the angles mentioned previously. These breaks occur at different cluster sizes for different compounds, i.e., $i = 4$ for $Zn_iSe_i$ and $Zn_iTe_i$, $i = 5$ for $Zn_iS_i$ and $Cd_iO_i$, and $i = 7$ for $Zn_iO_i$. In the zinc compounds, the break of planarity occurs at a smaller size as the X moves down in the periodic table. In other words, the larger the size of X, the more difficult it is to achieve linear angles. The larger size of the Cd atom, with respect to the Zn atom, explains why the break occurs at a smaller size for CdO rings, compared to ZnO clusters.

Rings are the global minima structures for small clusters, whereas three-dimensional structures are the global minima for larger clusters. These structures have been observed to be spheroids, distorted spheroids, and clustertubes. In most cases, spheroids are the global minima, except for $Cd_8O_8$, $Cd_9O_9$, and $Zn_8O_8$, where clustertubes are observed to be the global minima. In the case of $Zn_iX_i$ ($i = 7$, X = S, Se, Te), distorted spheroids are the global minima; structures similar to $Cd_7O_7^{D(I)}$ are the global minima for X = S, Se, and structures similar to $Cd_7O_7^{D(II)}$ are the global minima in the case of X = Te.

**3.3. Cohesive Energies.** Elsewhere, it has been demonstrated[58] that many cluster properties, according to the liquid drop model, lie within lines when plotted versus the inverse cube root of $i$ ($i^{-1/3}$). The cohesive energy is one of these properties. The cohesive energy per $Cd_iO_i$ unit is calculated according to eq 1:

$$E_f = \frac{iE_{Cd} + iE_O - E_{Cd_iO_i}}{i} \quad (1)$$

where $i$ is the number of CdO units. Theoretical and experimental observations for $Si_i$ clusters[59] show that clusters belonging to the same family lie within a line. The family lying above is the most stable family in that cluster size range. The cohesive energies of the three families of $Cd_iO_i$ clusters ($i = 3−15$)—namely, rings, spheroids, and clustertubes—are plotted versus $i^{-1/3}$ in Figure 5.

The points that can be observed to correspond to the ring structures tend to lie in a line with smaller slope than those of the spheroid and clustertube points. For small clusters, the ring line lies above the spheroid and clustertube lines; however, at $i = 8$, there is a crosing of lines and the clustertube line lies above the ring line and the spheroid line. Another crossing is found at $i = 12$, where the slope of the clustertube line becomes smaller and spheroid line lies above both the ring line and the clustertube line.

Fitting a line to the spheroid points, and extrapolating it to $i^{-1/3} = 0$, the theoretical value for the cohesive energy of the bulk can be obtained. The predicted cohesive energy is 550.88
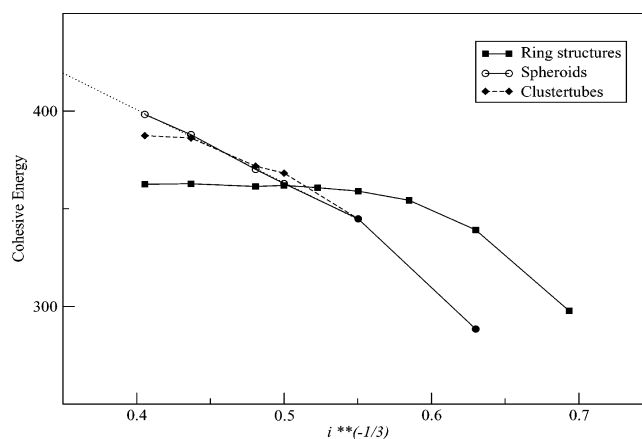


**Figure 5.** Cohesive energies (given in kJ/mol) for ring, spheroid, and clustertube structures.

kJ/mol. The experimental value is calculated according to the CODATA data[60] by eq 2:

$$E_{f,exp} = |\Delta H°_f(CdO) - \Delta H°_f(Cd) - \Delta H°_f(O)| - RT \quad (2)$$

which is 616.9 kJ/mol. The theoretical and experimental values fit well, although the clusters used in this extrapolation have a coordination number of three, not six, as the bulk does. This fit is consistent with our prediction of the global minima structures, because there is no space above this line in this cluster-size region for another cluster family. Nevertheless, this family (or families) is expected to be dominant in the region of larger cluster sizes. The diameter of the $Cd_{15}O_{15}$ spheroid is 0.85 Å, whereas the smallest group II−VI nanoparticle found experimentally has a diameter of 0.90 Å. This particle is thought to have a bulklike structure. Therefore, the transition to a family of clusters with a coordination number larger than three is approximately this cluster size. Further calculations are planned to find these transitions.

## 4. Conclusions

The lowest energy minima of the $Cd_iO_i$ clusters studied in the present work have been found to undergo a transition from a ring structure to a three-dimensional structure. This behavior parallels that of the previously investigated $Zn_iX_i$ clusters, where X = O, S, Se, Te.

The structural transition previously referenced results from a delicate balance between two opposite tendencies. On one hand, rings are favored by the tendency to linearity of the O−Cd−O bonds and, on the other hand, three-dimensional structures are favored by the tendency of achieving higher coordination. Our calculations indicate that the former dominates when the higher coordination does not carry too much strain for the bond angles. This occurs at $i = 8$ for $Cd_iO_i$ and $Zn_iO_i$, and at $i = 6$ for $Zn_iX_i$ (X = S, Se, Te). Naturally, the smaller size of the O valence orbitals accounts for its transition occurring at higher cluster sizes for $Y_iO_i$ (Y = Zn, Cd).

The predicted structures of the lowest-energy three-dimensional spheroid structures of $Cd_iO_i$, can be envisioned as being built of smaller basic building units, namely, the $Cd_2O_2$ squares and $Cd_3O_3$ hexagons. These structures seem to be the basic structural units for larger clusters in the same sense that $C_5$ pentagons and $C_6$ hexagons constitute the basic structural units of fullerenes.

According to the cohesive energies, these spheroids are the true global minima for cluster sizes of $i > 9$. The transition to cluster structures that have larger coordination numbers is

Clusters of Group II−VI Materials: Cd$_i$O$_i$ ($i \leq 15$)

*J. Phys. Chem. A, Vol. 107, No. 46, 2003* **9923**

predicted to happen for cluster sizes of $i > 16$. In the cluster-size region of $i = 3-7$, the rings are the most stable structures; in the region of $i = 8-9$, clustertubes are the dominant ones.

These spheroids could be used in the design of molecular-based solids (for instance, as in fullerites). To accomplish this, further theoretical work is required.

**References and Notes**

(1) Chu, T. L.; Chu, S. S. *Solid-State Electron.* **1995**, *38*, 533.
(2) Halliday, D. P.; Eggleston, J. M.; Durose, K. *Thin Solid Films* **1998**, *322*, 314.
(3) Yamamoto, T.; Toyama, T.; Okamoto, H. *Jpn. J. Appl. Phys.* **1998**, *37*, L916.
(4) Lee, J. H.; Lee, H. Y.; Park, Y. K.; Shin, S. H.; Park, K. J. *Jpn. J. Appl. Phys.* **1998**, *37*, 3357.
(5) Singh, V. P.; McClure, J. C.; Lush, G. B.; Wang, W.; Wang, X.; Thompson, G. W.; Clark, E. *Sol. Energy Mater. Sol. Cells* **1999**, *59*, 145.
(6) Burgelman, M.; Nollet, P.; Degrave, S. *Appl. Phys. A* **1999**, *69*, 149.
(7) Durose, K.; Edwards, P. R.; Halliday, D. P. *J. Cryst. Growth* **1999**, *197*, 733.
(8) Contreras, G.; Vigil, O.; Ortega, M.; Morales, A.; Vidal, J.; Albor, M. L. *Thin Solid Films* **2000**, *361−362*, 378.
(9) Chakrabarti, R.; Dutta, J.; Bandyopadhyay, S.; Bhattacharyya, D.; Chaudhuri, S.; Pal, A. K. *Sol. Energy Mater. Sol. Cells* **2000**, *61*, 113.
(10) Edwards, P. R.; Galloway, S. A.; Durose, K. *Thin Solid Films* **2000**, *361−362*, 364.
(11) Sebastian, P. J.; Ocampo, M. *Sol. Energy Mater. Sol. Cells* **1996**, *44*, 1.
(12) Hoffman, A. J.; Mills, G.; Yee, H.; Hoffmann, M. R. *J. Phys. Chem.* **1992**, *96*, 5546.
(13) Kuwabata, S.; Nishida, K.; Tsuda, R.; Inoue, H.; Yoneyama, H. *J. Electrochem. Soc.* **1994**, *141*, 1498.
(14) Corcoran, E. *Sci. Am.* **1990**, *263*, (11), 74.
(15) Schroer, P.; Kruger, P.; Pollmann, J. *Phys. Rev. B* **1993**, *47*, 6971.
(16) Schroer, P.; Kruger, P.; Pollmann, J. *Phys. Rev. B* **1993**, *48*, 18264.
(17) Schroer, P.; Kruger, P.; Pollmann, J. *Phys. Rev. B* **1994**, *49*, 17092.
(18) Vogel, D.; Kruger, P.; Pollmann, J. *Phys. Rev. B* **1995**, *52*, 14316.
(19) Pollmann, J.; Kruger, P.; Rohlfing, M.; Sabisch, M.; Vogel, D. *Appl. Surf. Sci.* **1996**, *104/105*, 1.
(20) Vogel, D.; Kruger, P.; Pollmann, J. *Phys. Rev. B* **1996**, *54*, 5495.
(21) Muilu, J.; Pakkanen, T. A. *Surf. Sci.* **1996**, *364*, 439.
(22) Muilu, J.; Pakkanen, T. A. *Phys. Rev. B* **1994**, *49*, 11185.
(23) Shou-heng, S.; Chuan, S.; Fink, K.; Staemmler, V. *Chem. Phys.* **2003**, *287*, 183.
(24) Kamat, P. V.; Bedja, I.; Hotchandani, S. *J. Phys. Chem.* **1994**, *98*, 9137.
(25) Freemantle, M. *Chem. Eng. News* **1999**, *77*, 13.
(26) Ecker, A.; Weckert, E.; Schnockel, H. *Nature* **1997**, *387*, 379.
(27) Rousseau, R.; Dietrich, G.; Kruckeberg, S.; Lutzenkirchen, K.; Marx, D.; Schweikhard, L.; Walther, C. *Chem. Phys. Lett.* **1998**, *295*, 41.
(28) Cizeron, J.; Pileni, M. P. *J. Phys. Chem. B* **1997**, *101*, 8887.
(29) Gurin, V. S. *J. Phys. Chem.* **1996**, *100*, 869.

(30) Guo, B.; Kerns, K.; Castleman, A. *Science* **1992**, *255*, 1411.
(31) Guo, B.; Wei, S.; Purnell, J.; Buzza, S.; Castleman, A. *Science* **1992**, *256*, 515.
(32) Xue-yin, J.; Yan, J.; Zhi-lin, Z.; Shao-hong, X. *J. Cryst. Growth* **1998**, *191*, 692.
(33) Walther, C.; Dietrich, G.; Dostal, W.; Hansen, K.; Krückeberg, S.; Lützenkirchen, K.; Schweikhard, L. *Phys. Rev. Lett.* **1999**, *83*, 3816.
(34) Fowler, J. E.; Ugalde, J. M. *Phys. Rev. A* **1998**, *58*, 383.
(35) Tomasulo, A.; Ramakrishna, M. V. *Chem. Phys.* **1996**, *210*, 55.
(36) Fuentealba, P.; Reyes, O. *J. Phys. Chem. A* **1999**, *103*, 1376.
(37) Haeser, M.; Schneider, U.; Ahlrichs, R. *J. Am. Chem. Soc.* **1992**, *114*, 9551.
(38) Lou, L.; Guo, T.; Nordlander, P.; Smalley, R. E. *J. Chem. Phys.* **1993**, *99*, 5301.
(39) Yu, W. W.; Peng, X. *Angew. Chem., Int. Ed.* **2002**, *41*, 2368.
(40) Katari, J. E.; Colvin, V. L.; Alivisatos, A. P. *J. Phys. Chem.* **1994**, *98*, 4109.
(41) Wang, Y. A.; Li, J. J.; Chen, H.; Peng, X. *J. Am. Chem. Soc.* **2002**, *124*, 2293.
(42) Qu, L.; Peng, X. *J. Am. Chem. Soc.* **2002**, *124*, 2049.
(43) Peng, Z. A.; Peng, X. *J. Am. Chem. Soc.* **2002**, *124*, 3343.
(44) Pesika, N. S.; Hu, Z.; Stebe, K. J.; Searson, P. C. *J. Phys. Chem. B* **2002**, *106*, 6985−6990.
(45) Matxain, J. M.; Fowler, J. E.; Ugalde, J. M. *Phys. Rev. A* **2000**, *61*, 512.
(46) Matxain, J. M.; Fowler, J. E.; Ugalde, J. M. *Phys. Rev. A* **2000**, *62*, 553.
(47) Matxain, J. M.; Mercero, J. M.; Fowler, J. E.; Ugalde, J. M. *Phys. Rev. A* **2000**, *64*, 053201.
(48) Behrman, E. C.; Foehrweiser, R. K.; Myers, J. R.; French, B. R.; Zandler, M. E. *Phys. Rev. A* **1994**, *49*, 1543.
(49) Becke, A. D. *J. Chem. Phys.* **1993**, *98*, 5648.
(50) Hohemberg, P.; Kohn, W. *Phys. Rev.* **1964**, *136*, 3864.
(51) Lee, C.; Yang, W.; Parr, R. G. *Phys. Rev. B* **1988**, *37*, 785.
(52) Becke, A. D. *Phys. Rev. A* **1988**, *38*, 3098.
(53) Stevens, W. J.; Krauss, M.; Basch, H.; Jasien, P. G. *Can. J. Chem.* **1992**, *70*, 612.
(54) Schmidt, M. W.; Baldridge, K. K.; Boatz, J. A.; Elbert, S. T.; Gordon, M. S.; Jensen, J. J.; Koseki, S.; Matsunaga, N.; Nguyen, K. A.; Su, S.; Windus, T. L.; Dupuis, M.; Montgomery, J. A. *J. Comput. Chem.* **1993**, *14*, 1347−1363.
(55) Stewart, J. J. P. *J. Comput. Chem.* **1991**, *12*, 320.
(56) Frisch, M. J.; Trucks, G. W.; Schlegel, H. B.; Scuseria, G. E.; Robb, M. A.; Cheeseman, J. R.; Zakrzewski, V. G.; Montgomery, J. A., Jr.; Stratmann, R. E.; Burant, J. C.; Dapprich, S.; Millam, J. M.; Daniels, A. D.; Kudin, K. N.; Strain, M. C.; Farkas, O.; Tomasi, J.; Barone, V.; Cossi, M.; Cammi, R.; Mennucci, B.; Pomelli, C.; Adamo, C.; Clifford, S.; Ochterski, J.; Petersson, G. A.; Ayala, P. Y.; Cui, Q.; Morokuma, K.; Malick, D. K.; Rabuck, A. D.; Raghavachari, K.; Foresman, J. B.; Cioslowski, J.; Ortiz, J. V.; Stefanov, B. B.; Liu, G.; Liashenko, A.; Piskorz, P.; Komaromi, I.; Gomperts, R.; Martin, R. L.; Fox, D. J.; Keith, T.; Al-Laham, M. A.; Peng, C. Y.; Nanayakkara, A.; Gonzalez, C.; Challacombe, M.; Gill, P. M. W.; Johnson, B. G.; Chen, W.; Wong, M. W.; Andres, J. L.; Head-Gordon, M.; Replogle, E. S.; Pople, J. A. *Gaussian 98*, revision A.7; Gaussian, Inc.: Pittsburgh, PA, 1998.
(57) HyperChem, Release 4.5 for Windows, Molecular Modeling System, Hypercube, Inc., 1994, 1995.
(58) Jortner, J. *Z. Phys. D, At., Mol. Clusters* **1992**, *24*, 247.
(59) Hartke, B. *Angew. Chem., Int. Ed.* **2002**, *41*, 1468−1487 and references therein.
(60) Lide, D. R., Ed. *CRC Handbook of Chemistry and Physics,* 79th ed.; CRC Press: Boca Raton, FL, 1998−1999; pp 5−24.